FUNDAMENTALS & APPLICATIONS

CHEMELECTROCHEM

ANALYSIS & CATALYSIS, BIO & NANO, ENERGY & MORE

Accepted Article

Title: Biologically-induced hydrogen production drives high rate / high efficiency microbial electrosynthesis of acetate from carbon dioxide

Authors: Ludovic Jourdin; Yang Lu; Victoria Flexer; Jurg Keller; Stefano Freguia

To be cited as: ChemElectroChem 10.1002/celc.201500530

Link to VoR: http://dx.doi.org/10.1002/celc.201500530

A Journal of

ChemPubSoc Europe

www.chemelectrochem.org

WILEY-VCH

FULL PAPER WILEY-VCH

Biologically-induced hydrogen production drives high rate / high efficiency microbial electrosynthesis of acetate from carbon dioxide

Ludovic Jourdin,*[a,b, †] Yang Lu,[a] Victoria Flexer,[a, ‡] Jurg Keller,*[a] and Stefano Freguia[a,b]

Abstract: Electron transfer pathways occurring in biocathodes are still unknown. We demonstrate here that high rates of acetate production by microbial electrosynthesis are mainly driven by an electron flux from the electrode to carbon dioxide, occurring via biologically-induced hydrogen, with 99 ± 1% electron recovery into acetate. Nevertheless, acetate production is shown to occur exclusively within the biofilm. The acetate-producers, putatively *Acetoanaerobium*, showed the remarkable ability to consume a high H_2 flux before it could escape from the biofilm. At zero wastage of H_2 gas, it allows superior production rates and lesser technical bottlenecks over technologies that rely on mass transfer of H_2 to microorganisms suspended in aqueous solution. This study suggests that bacterial modification of the electrode surface (possibly via synthesis of Cu nanoparticles) is directly involved in the significant enhancement of the hydrogen production.

Introduction

The threat of global warming, diminishing fossil fuel resources and our society's high energy and commodity chemicals demands are creating a rapidly growing demand for new, sustainable forms of fuels and chemicals. Microbial electrosynthesis (MES) of organics from carbon dioxide has been recently put forward as an attractive technology for the renewable production of valuable multi-carbon reduced end-products[1] and as a promising CO_2 transformation strategy over current techniques.[2, 3] MES uses electrical current as a driving force, which electroactive microorganisms convert to the reduction of carbon dioxide to organics.[4] Intermittent renewable electrical energy sources such as solar and wind can be considered as appropriate options to power MES processes.[5]

Microbial electrosynthesis has now been studied at lab-scale in several groups over the past few years.[2, 5-20] In most studies using mixed microbial cultures, acetate was found to be the main end-product from CO_2 when methanogenesis was inhibited.[6-10, 12-14] Ganigue et al. (2015), however, reported the concomitant production of butyrate, acetate, butanol and ethanol from CO_2.[2] Few studies have now shown that high MES performance can be reached.[6, 10] In one of our previous study[6] we reported a high biocathode current density of up to -102 A m^{-2} (equivalent to ca. -9960 A $m^{-3}_{electrode}$ when normalized to the electrode volume) with a concurrent acetic acid production rate of 685 ± 30 g m^{-2} day^{-1} (equivalent to 66 kg $m^{-3}_{electrode}$ day^{-1} and 98 kg_{CO2} $m^{-3}_{electrode}$ day^{-1} captured). The CO_2 and electron recovery in this study was up to 98 ± 3 % into the final product (product yield) and a high acetic acid titer of up to 11 g L^{-1} could be reached. This was possible thanks to the combination of a well acclimatized and highly performing microbial culture[6] (very fast start-up after culture transfer), coupled with the use of a newly synthesized electrode material[6] (multiwalled carbon nanotubes deposited on reticulated vitreous carbon by electrophoretic deposition, called EPD-3D). That study showed that industrial production process standards, such as fermentation-type volumetric production rate and product yield, can be reached by microbial electrosynthesis of organics from CO_2, though there are still several issues to be overcome for the actual bioelectrochemical system (BES) technology scale-up and practical implementation. In this regard, a more in-depth and fundamental understanding of the process and particularly on how electrons flow from the cathode to the terminal electron acceptor is still missing, even though it may be of paramount importance (e.g. for improved reactor design).

To date, mostly anodic microbial processes and anodic extracellular electron transfer (EET) mechanisms have been extensively investigated. Three main types of EET pathways have been identified.[21] The first two involve electron transfer chain components of the microbes being in direct contact with the electrode surface and referred to as direct electron transfer (DET), either through membrane bound electron transport proteins such as cytochromes or along conductive pili. The third pathway involves electron mediators serving as electron carriers due to their ability to reversibly be oxidized and reduced between the electrodes and the microorganisms, which is referred to as mediated electron transfer (MET).

Information on the reverse process, i.e. electron flow from electrodes (cathodes) towards the terminal electron acceptor, is very limited. Until now, the exact cathodic electron transfer pathways are still unknown. Several potential mechanisms similar to those occurring at bioanodes, but operating at different redox potentials, have been proposed.[1, 22-24] In the context of microbial electrosynthesis from carbon dioxide, potential

[a] Dr. L. Jourdin, Dr. Y. Lu, Dr. V. Flexer, Prof. J. Keller, Dr. Stefano Freguia
Advanced Water Management Centre
University of Queensland
Gehrmann building, level 4, 4072 Brisbane, QLD, Australia
E-mail: ludovic.jourdin@wur.nl, j.keller@awmc.uq.edu.au
[b] Dr. L. Jourdin, Dr. Y. Lu, Dr. Stefano Freguia
Centre for Microbial Electrochemical Systems
University of Queensland
Gehrmann building, level 4, 4072 Brisbane, QLD, Australia
E-mail: ludovic.jourdin@wur.nl
[†] Dr. L. Jourdin
Present address: Sub-department of Environmental Technology
Wageningen University
Axis-Z, Bornse Weilanden 9, 6708 WG, Wageningen, the Netherlands
[‡] Dr. V. Flexer
Present address: Centro de Investigaciones y Transferencia-Jujuy-Conicet
Av. Bolivia 1239, San Salvador de Jujuy, 4600, Argentina

Supporting information for this article is given via a link at the end of the document.

mechanisms of electron transfer from the cathode have been discussed by several groups[2, 14, 20, 25] with the possibility of at least part of the electrons being transported to the acetogenic bacteria via hydrogen which is either abiotically or biologically produced. However, there is a clear lack of experimental evidence towards these H_2-mediated electron transfer assumptions. Additionally, other electron transfer mechanisms such as DET or through other electron shuttles could not be ruled out from those studies.

In this study, the titration and off-gas analysis (TOGA) sensor developed by Pratt et al. (2002)[26] was modified to allow the online measurement of gaseous products (i.e. H_2, CH_4, CO_2) from bioelectrochemical systems (BESs).[27] Different tests were carried out (e.g. chronoamperometry and linear sweep voltammetry with and without carbon dioxide) on both biotic BESs for microbial electrosynthesis of acetate from carbon dioxide and abiotic BESs lacking the microorganisms (pure electrochemical reactions) using the TOGA sensor. In addition, microorganisms involved in the process were identified and the relative importance of both biofilm and planktonic cells in terms of overall process performance was investigated. We demonstrate for the first time experimentally that the CO_2 reduction to acetate is driven by biologically-induced hydrogen production at high rate (1.15 m^3_{H2} $m^{-2}_{electrode}$ day^{-1}) with ca. 99 ± 2% of total supplied electrons recovered into acetate (at a high production rate of ca. 685 g m^{-2} day^{-1}) in the presence of CO_2.

Results and Discussion

A high rate microbial electrosynthesis reactor, equipped with EPD-3D 45ppi synthetized by electrophoretic deposition as biocathode material, which was run in fed-batch mode for 70 days as previously described[6], was used in this study. After this long-term chronoamperometry test at -0.85 V vs. SHE, the reactor was set up to be used in combination with the TOGA sensor as described in the materials and methods section. Throughout all the tests, no methane was detected. The H_2 flow rate could be determined, and the corresponding current consumed into H_2 as an end-product was calculated. The tests described below were also run on an identical duplicate reactor (as indicated in the text), equipped with a EPD-3D 60 ppi biocathode electrode using the exact same setup and experimental conditions and showing high MES rate. Results obtained on both duplicate reactors are in very close agreement. Representative TOGA results obtained on the duplicate reactor can be seen in the Supporting Information while microbial community analysis, SEM and EDS results from both replicates can be seen below. All data points in the figures have been normalized to the projected surface area of the electrode; way of normalization extensively discussed previously.[6, 10] Reported values in the text have also been normalized to projected surface area unless otherwise specified.

MES of acetate driven by biologically-induced hydrogen production

After 25 days of acclimation to the new setup and experimental conditions, the TOGA sensor was used alternatively with and without carbon dioxide fed. The total current consumed and the current assimilated into hydrogen as end-product over time can be seen in Figure 1. The TOGA sensor also allowed confirming that no methane was produced during the course of the experiment (data not shown). Liquid samples were also taken at the beginning and end of each period, and volatile fatty acid concentrations were monitored.

It can be observed that essentially no H_2 was detected from the reactor when CO_2 was continuously fed to the reactor. VFA analysis also showed that acetate was the sole product and that about 99 ± 1% of the total electrons consumed were assimilated into acetate (averaged on both periods with CO_2 showed in Figure 1 and between the two replicate reactors; as a representative result obtained on the duplicate reactor in presence of CO_2, please refer to the left side of Figure S1, before cells in suspension were removed, where it can also be observed that no or very small traces of H_2 were detected). This confirms observations made in previous studies on fed-batch reactors fed with bicarbonate as an inorganic carbon source.[6, 10] However, the notable difference is that in this case, gases ($He:CO_2$) were continuously bubbled through the reactor, and any hydrogen that would be produced and not directly consumed would be stripped out due to its low solubility in water. Remarkably, it can be seen that when CO_2 was removed, i.e. pure He was sparged (referred to as without CO_2 in Figure 1 and the following discussion), no current decrease was observed and electron recovery into H_2 as the end-product went up to 95 ± 3% (averaged between both duplicates). This indicates that the electron flux from the electrode to the terminal electron acceptor, CO_2, when present, occurs mostly through hydrogen. Indeed, if direct electron transfer from the electrode to the acetate-producer microorganisms was occurring, a decrease in current consumed would be expected in the absence of CO_2.

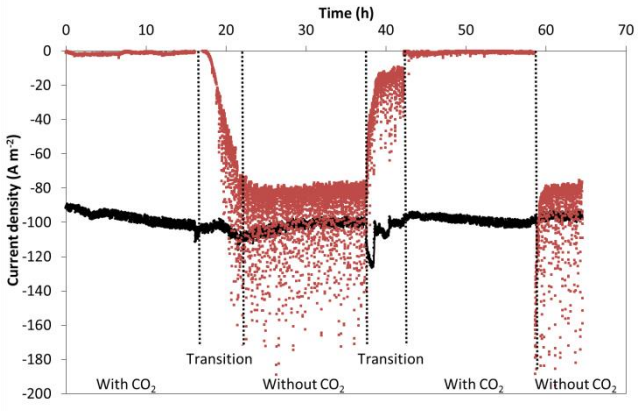

Figure 1. Chronoamperometry test with the TOGA sensor with and without CO_2 fed, at -0.85 V vs. SHE applied cathode potential and pH 6.7. The solid black line represents the total current consumed while the red dotted line represents the current consumed into hydrogen (more negative values represent higher hydrogen production). The current values were normalized to projected surface area.

Moreover, acetate concentration was found to remain constant in the absence of CO_2, i.e. it was not consumed despite being the sole carbon source present in the system. This confirms that the enriched active microbial community is purely autotrophic, even though fairly high concentration of acetate had been present in the reactor for more than 100 days (including the previous fed-batch experiment). This was expected, as methanogens were inhibited and no other electron acceptor was present in the system. The first transition period indicated in Figure 1 corresponds to the time it took to remove all the dissolved CO_2 and HCO_3^- (i.e. the equilibrium was shifted towards CO_2 until its complete disappearance) as monitored with the TOGA sensor. The second transition period represents the progressive CO_2 saturation of the catholyte medium and the potential lag time it took the microbial consortium to recover its full activity, i.e. CO_2 conversion to acetate.

Around days 30 to 35, linear sweep voltammograms (LSVs) both with and without CO_2 fed were measured (on both replicates) and representative plots can be seen in Figure S2. They confirmed the observations made above during chronoamperometry tests, with no H_2 being detected in the presence of CO_2, while all electrons consumed were assimilated into H_2 in the absence of CO_2. Both chronoamperometry and LSV tests with the TOGA sensor connected were also performed on an identical EPD-3D 45ppi abiotic control setup, but without the microbial inoculum, and are shown in Figure S3 and S2 A and B, respectively. Significantly lower, and constant, current density of about -2 A m^{-2} was recorded throughout the chronoamperometry test at -0.85 V vs. SHE, compared to the current density of about -100 A m^{-2} recorded in the biocathode (using the same EPD-3D electrode material). Even at this low current the TOGA sensor was able to detect that all the electrons were directed towards H_2 production only, in the abiotic control, during both the chronoamperometry and LSV tests.

Unlike other studies that generally report H_2 diffusion losses hence are unable to close electron balances at low current[28, 29], the TOGA sensor allows us to close the electron balance to within 1% in this study. As previously reported, a significant shift of the reductive wave towards higher potentials was observed on the biocathodes compared to the abiotic control., with the same onset potential of the reductive wave in presence and absence of CO_2. This experimentally confirms hypotheses made by others so far[14, 16, 30], that the shift of the reductive wave is due to an increase in (bio)catalytic activity and not due to the reaction equilibrium being shifted due to hydrogen consumption (thermodynamic). The combination of LSVs, both with and without CO_2 fed, with the TOGA sensor confirms that this increase in catalytic activity is directed towards higher H_2 production rates. Moreover, the significantly lower current density recorded in the abiotic control indicated that abiotically produced H_2 cannot account for all the H_2 and acetate produced without and with CO_2 fed, respectively, in the biocathode system. Therefore, the hydrogen production must be biologically-induced.

Highly specific microbial enrichment

Microbial community structures are summarized in the network plot (Figure 2) between samples (shown as filled ellipses) from the two duplicate reactors (top and bottom, respectively) and top operational taxonomic units (OTUs; >10% relative abundance, labelled with classification in the boxes). Presence of OTUs is indicated by arrows pointing to the sample node. The width of linking arrows and position of OTUs reflect the abundance contribution (thicker and closer as higher contribution). Microbial communities were consistent between duplicates. Biofilm communities were enriched up to 75% of top OTUs from a diverse initial community (Figure S4[16]), emphasizing that the peculiar experimental conditions allowed for a specific microbial selection.

Microbial community of replicate biofilm samples were consistent with even distribution of *Acetoanaerobium*, *Hydrogenophaga*, *Methanobrevibacter* and one New Reference_OTU. *Acetoanaerobium* is an anaerobic bacterium that has been reported in the past for its ability to produce acetate from CO_2 and H_2.[31] Remarkably, *Acetoanaerobium* was mainly dominant in the biofilm and present in suspension at only a low abundance. The New Reference_OTU (Figure 2) was classified within phylum Firmicutes with *Acetoanaerobium noterae* as the top hit classification (89% similarity) and may be related to acetate generation in this condition.

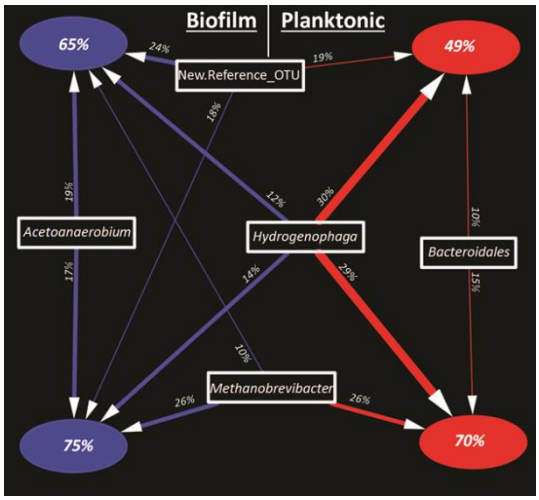

Figure 2. Network between samples (biofilm (left) and planktonic (right), respectively) from the two duplicate reactors (top and bottom, respectively) and top OTUs. Sample nodes are shown as filled ellipse labelled with total abundance of top OTUs (>10%). OTU nodes are labelled with classificatoin in the rectangles. Linkage between OTUs and samples are indicated by arrows. The width of the arrows reflects the abundance of OTU as labelled. Network regarding to biofilm and planktonic community are shown in blue and red respectively

Hydrogenophaga was found abundant in suspension (ca. 30%) and also at fairly high abundance (ca. 13%) in the biofilm. To the best of our knowledge, *Hydrogenophaga* has only been reported as a facultative autotrophic hydrogen-oxidizing bacteria.[32] It was

isolated from anodic biofilms of acetate-fed microbial fuel cells[33] and speculated to work in close syntrophy with acetate-oxidizer *Geobacter* as hydrogen-utilizing exoelectrogen, hence directly transferring electrons to the electrode.[34] *Hydrogenophaga* was also reported to be a key player in autotrophic biofilms active in denitrification.[35, 36] However, the actual function of *Hydrogenophaga* under these peculiar biocathode conditions requires further investigation. *Methanobrevibacter* was also found abundant, though methanogenic activity was suppressed by the addition of bromoethanesulfonate and methane was not detected throughout the course of the experiment (Figure 2). Previous studies suggested that hydrogenotrophic methanogens could also conserve energy by reducing proton to hydrogen.[37, 38] We could speculate that *Methanobrevibacter* may catalyze H_2 production in these biocathode conditions, however more in-depth investigation is needed to shed light on its function.

MES of acetate exclusively occurs within the biofilm

The relative abundance of these key biofilm microorganisms, except hydrogenophaga, dropped in the community in suspension, highlighting the likely major importance of the biofilm in relation to the process performance. To confirm this hypothesis, the planktonic cells were removed by replacing the whole catholyte suspension with fresh, cell-free catholyte solution. Chronoamperometry tests with the TOGA sensor connected were performed before and after the planktonic cell removal and can be seen in Figure 3.

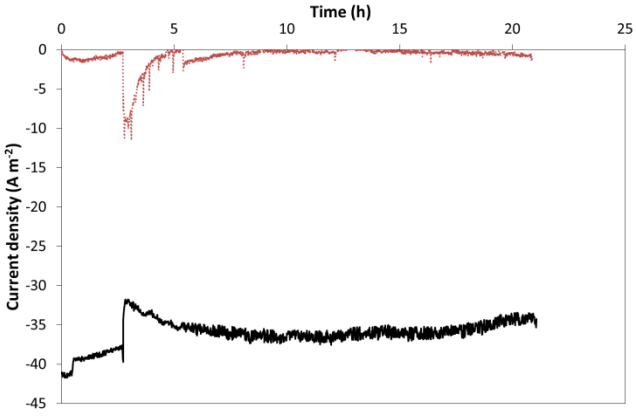

Figure 3. Chronoamperometry test with the TOGA sensor, in the presence of CO_2, at -0.85 V vs. SHE applied cathode potential and pH 6.7 before and after planktonic cells removal (represented by the vertical dotted line). The solid black line represents the total current consumed while the red dotted line represents the current consumed into hydrogen. The current values were normalized to projected surface area.

Similar current densities were recorded before and after the planktonic cells were removed and still about 100% of the electrons consumed were assimilated into acetate after the medium was replaced. This confirms the paramount importance of the biofilm in the MES performance.

It can be noticed that the current densities in Figure 3 are lower than those in Figure 1. This reflects a progressive decrease over time of the reactor current density as shown in Figure S5. We speculate that the repeated recording of many LSVs may have affected the performance of this biocathode, as corroborated by further experiments as described below (see Figure 6). Therefore, we repeated this planktonic cell removal experiment on the fully active 60 ppi EPD-3D duplicate biocathode, on which no LSV was performed, and the results can be seen in Figure S6. Similarly, it can be seen that the current remained constant after the planktonic cells were removed, even at the very high current density of around -100 A m^{-2}, and that H_2 was not detected either, hence all the electrons were assimilated into acetate, as confirmed by VFA analysis. Before planktonic cells removal, a qualitative test was performed. H_2 was fed in-situ via electrolysis on a platinum wire inserted in the cathode chamber while CO_2 was fed and no cathodic potential was applied. This led to acetate production, confirming that hydrogen does indeed drive the reaction (data not shown).

As described above, the main electron transfer to the acetogens occurs through biologically-induced hydrogen. This shows the quite extraordinary capability of the acetogens to consume such a high H_2 flow rate (1.15 m^3_{H2} m^{-2} day^{-1}) within the biofilm, without the H_2 able to escape from it (and hence be detected by the TOGA sensor). This finding is of high importance for the potential large-scale implementation of this technology and reactor design. Not only would high acetate production rates be desirable, but also the handling of extra hydrogen could be problematic and a technical challenge. The direct H_2 consumption within the biofilm is an opportunity and presents several advantages over other technologies that would rely on the mass transfer of H_2 molecules to microorganisms suspended in aqueous solution, such as the artificial photosynthetic system proposed by Jian Yu (2014).[39] That system comprises a photovoltaic assembly which generates electricity to drive a water electrolyser for the formation of H_2 which is introduced in a type of dark-fermenter in which H_2-oxidizing bacterial cells assimilate CO_2 to form bio-based products.[39] High gas feed rates and superficial gas velocities while avoiding H_2 wastage are needed for efficient mass transfer and consumption and for economic viability and operational safety. However, the very low solubility of H_2 (1.26 mmol L^{-1} atm^{-1}) poses a technical challenge to maintaining a high mass transfer in large bioreactors, without substantial loss of H_2.[39] Comparatively, the system described here allows combining both H_2 production and CO_2 assimilation to a bio-based product, acetate, within a unique microbial electrosynthesis reactor, without H_2 waste and extra-handling needed. Additionally, significantly lower acetate production rates of 0.006 to 0.01 g L^{-1} h^{-1} from microbiomes supplied with H_2 and CO_2 have been reported [40, 41] when compared to rates obtained here with MES.[6] Moreover, it was shown that if supplied with sufficient H_2 and CO_2, autotrophic H_2-oxidizing bacterial growth can be very-fast, comparable to heterotrophic growth.[39, 42, 43] It was concluded that the microbial metabolism of the gases was not the limiting factor, but that maintaining an appropriate mass transfer rate of the gases to the microorganisms was actually the technical bottleneck of autotrophic technologies such as the dark fermenters described above.[39] This could also partly explain the

observation made in our previous study, showing very fast start-up of MES biocathode inoculated with an enriched culture.[6]
Blanchet et al. (2015)[25] also recently reported on the importance of hydrogen in the conversion of CO_2 to acetate but in a different process than reported here. They investigated CO_2 conversion purely occurring via cells in suspension, with no biological catalytic activity recorded on the electrode (showed by chronoamperometry and CV experiments) and purely abiotic hydrogen delivered by either stainless steel electrode or directly from a gas cylinder; a process referred to as a type of dark fermentation by several before, as discussed above. This process is indeed very relevant and also deserves much attention. They interestingly reported that an electrode was a more efficient hydrogen sparger than a simple aquarium diffuser, with an electron/H_2 recovery into acetate of about 53% with H_2 delivered electrochemically (abiotic) and only about 13% when using a gas diffuser. They also rightfully pointed out that an MES reactor must operate at high current densities to be economically efficient, while arguing however that at high current densities, H_2 evolution would mechanically keep the microbial cells away from the electrode surface. We show here that biologically-induced H_2 (biological catalysis activity on the surface of the electrode), and its further conversion by acetogens within the biofilm, coupled with an efficient electrode material design could allow achieving high volumetric current densities while not removing the biofilm. This could also be a way worth pursuing for scaling-up microbial conversion of CO_2 to acetate. However, this study aimed at shedding light on the electron transfer mechanism occurring in MES reactors, and scaling up the technology was out of its scope and requires much more investigation.

High H_2 production capability unaffected by biofilm removal

We further investigated the high biologically-induced H_2 production capability of these biocathode systems by subjecting the biofilm to extreme conditions in order to remove it, as described in the Materials and Methods section. After each treatment, the electrode was reconnected and current recorded at the same applied potential of -0.85 V vs. SHE and is plotted in Figure 4.
The current density before those treatments was about -29 A m^{-2}. Remarkably, after the low pH treatment the current was still high, about -22 A m^{-2}. The TOGA sensor was used before and after the low pH step (Figure 4) and we can observe that the acetogens were successfully inhibited, or killed, by the low pH as H_2 was the sole product generated afterwards. Further sterilization and air treatment also did not significantly affect the H_2 production capability of the cathode, as the current density increased back up to about -20 A m^{-2} few days after the air-drying treatment. The low pH and autoclave treatments were repeated on the biocathode duplicate at high current density (ca. -100 A m^{-2} before treatments) and can be seen in Figure S6. We first confirmed that acetogens' activity after low pH was inhibited. But remarkably, the current after autoclaving was similar, ca. -110 A m^{-2} than before exposing the biocathode to those extreme conditions. The slightly lower current recorded after the low pH exposure was due to the reference electrode being faulty leading to an applied cathode potential of about -0.77 V vs. SHE instead. It has to be stressed here once again that the current recorded in the same conditions on an abiotic control was far lower (-2 A m^{-2}) and cannot account for this high H_2 production rate. We also confirmed that autoclaving a EPD-3D electrode does not affect its surface properties (e.g. its CNT layer), by recording the same current on an abiotic control before and after autoclave treatment (data not shown).

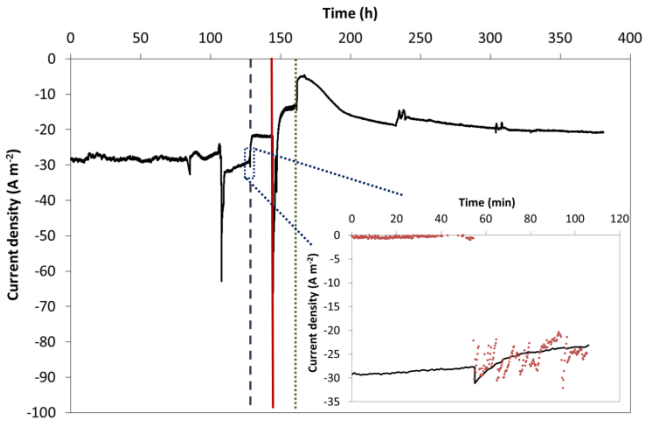

Figure 4. Chronoamperometry test with the TOGA sensor connected, in the presence of CO_2, at -0.85 V vs. SHE applied cathode potential. The vertical dashed, solid and dotted lines represent the time periods when pH was adjusted to 2 for 2-3 hours, the reactor and the recirculation bottle were autoclaved (and the rest of the setup sterilized with ethanol), and the electrode taken out of the reactor and left to dry in air for 1 week, respectively. During those three periods, current evolution over time was not recorded and all experimental results are collapsed as a continous result in this figure. The inset graph shows the current consumed into hydrogen (red dotted line) measured with the TOGA sensor during two distinct periods of the chronoamperometry test, before and after the low pH period (marked by the dashed line).

To further confirm these extreme treatments effectively removed the biofilm off the electrodes, SEM images were taken on both fully active biocathode biofilms and the electrodes that went through those treatments, from both duplicates, and representative images can be seen in Figure 5. Abiotic EPD-3D SEM images are also shown. FISH images of an active biocathode biofilm dispersed in solution have also been taken and are shown in Figure S7.

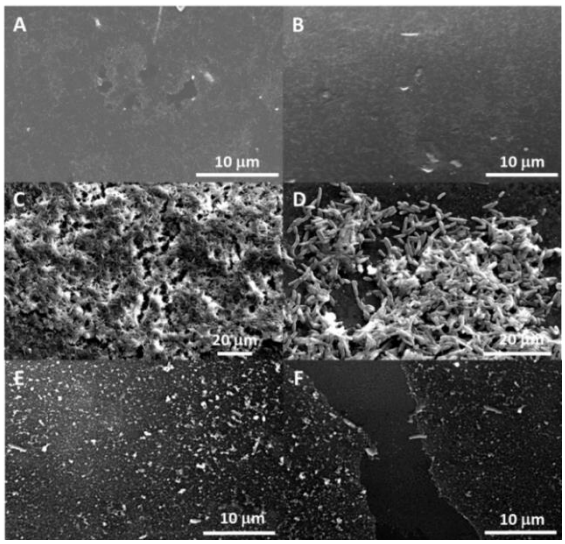

Figure 5. Scanning Electron Micrographs (SEM) images at different magnification of (A) and (B) bare EPD-3D abiotic control; (C) and (D) fully active EPD-3D biocathode biofilm; (E) and (F) EPD-3D biocathode after extreme conditions treatments (low pH, autoclave, air drying).

First of all, a predominant biofilm could be observed on the live biocathode electrode surface. Remarkably for a biocathode biofilm, it shows a biofilm of a few layers of microorganisms and of an approximate total thickness of 5-10 µm. This is relatively thin compared to anodic biofilms that have been reported at up to 100 µm.[44] However, to the best of our knowledge, previous biocathode studies generally reported microorganisms dispersed on electrode surfaces[11, 13] but rarely a well-established biofilm with entangled multi-layered microorganisms. This could be correlated to the high acetate production rates showed above and previously reported by us[6, 10], and the ability of the acetate-producers to consume this high rate of H_2 before it could escape from the biofilm. As previously reported, the special electrode surface characteristics with the nanoscale structure formed by the CNTs may favor microorganisms' attachment and biofilm development over its surface.[10] Comparatively, no biofilm could be observed on the electrodes that were subjected to extreme conditions, with only a few dispersed cells observed. Those were confirmed to be dead cells by FISH, by no or very few microorganism hybridizing with the general bacteria probes (*EUBmix*), as opposed to the active biocathode as visualized in Figure S7. *Acetoanaerobium*, believed to be at least one of the main acetate-producers as discussed above, were observed as long straight or curved rods up to 5 µm in size, whereas the *Betaproteobacteria*, mainly *Hydrogenophaga*, were shown to be small rods or cocci about 1µm in size. Those two different cell types appeared entangled together within the biofilm (Figure 5 C and D). In addition, we can observe on both the sterilized and active electrodes, some inorganic material deposited on the surface of the electrode, which is not observed on the abiotic control surface (Figure 5). This electrode surface 'modification' is hence showing to be permanent and not affected by the extreme sterilizations they were subjected to.

Bacterial surface modification directly involved in the significant H_2 production enhancement

To further investigate the cause of such high H_2 production performance, even after the biofilm was removed, cyclic voltammetry experiments were performed on both the bioactive and sterilized cathodes (duplicates) at pH 7 and representative plots are shown in Figure 6.

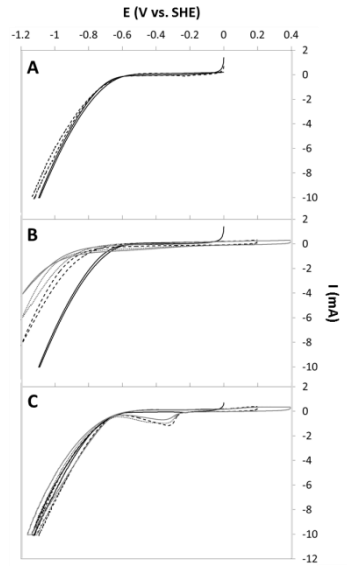

Figure 6. A) Cyclic voltammetry on both bioactive (solid line) and sterilized (dashed line) cathodes right after chronoamperometry at -0.85 V vs. SHE (also represented by solid black lines in B and C). B) CVs recorded on sterilized cathode and C) on bioactive cathode. Both cathodes were then electrochemically oxidized at +0.2 V vs. SHE for 30 min after which a CV was recorded (dashed black line). Following, CVs were recorded after further electrochemical oxidation at +0.2 V vs. SHE for 60 min (dotted grey line) and finally at +0.4 V vs. SHE for 30 min (solid grey line). CVs were recorded at pH 7 and 1 mV s^{-1} scan rate.

We can observe that the H_2 reductive wave onsets are very similar on both bioactive and sterilized cathodes after chronoamperometry at -0.85 V vs. SHE (Figure 6A). This confirms the observations made above and the similar current consumption towards H_2 production before and after extreme condition treatments. We can observe in Figure 6B however, that oxidative current from +0.2 V vs. SHE and above applied for a short period of time (30 to 60 min) irreversibly affected the cathode performance and H_2 production, with a progressive shift of the reductive wave towards lower potentials. This shows that the compound(s)/element(s) playing a key role in the H_2 production mechanism are irreversibly oxidized at higher potentials and performance is not recovered. Interestingly, the biofilm was shown to be able to reduce this compound back to its active form, from ca. -0.25 V vs. SHE, without affecting the H_2 reductive wave onset and H_2 production rate along the potentials range (Figure 6C). This further demonstrates the key role of the microorganisms in the high MES performance and significantly higher H_2 production capability reached after inoculation, compared to abiotic controls. Microorganisms seem to be

modifying the cathode surface with catalytically active redox species, which are resistant to high temperature and extreme pH, but are irreversibly lost or damaged through oxidation at positive potentials in the absence of bacteria.

In order to elucidate what redox active species is responsible for such an enhancement of the catalysis of H_2 evolution, the surface chemistry of both the bioactive and sterilized cathodes (duplicates) were analyzed by energy-dispersive X-ray spectroscopy (EDS). Several areas of each electrode were analyzed for reproducibility. All scans can be seen in Figure S8. As expected only carbon and oxygen elements are present on the surface of the abiotic control. In addition to C and O, Na, P, S, Cl and K were also detected on both the bioactive and sterilized cathode. Those elements are common and are believed not to play a role in H_2 catalysis. More surprisingly, a metal, copper (Cu), was detected in each sample, as showed in Figure 7 which is a zoom of the EDS scan around the area of interest. It was also confirmed that Cu was not detected on the abiotic control (Figure 7D).

Using the reported Pourbaix diagram (potential/pH diagram) of the copper system at similar dissolved concentration (1 μM) than used in this study[45], we confirmed that metal Cu gets oxidized at potentials higher than 0.05 V vs. SHE at pH 7 to another crystalline form, Cu_2O which is further oxidized to CuO above 0.25 V vs. SHE. This correlates with the observations made by CVs showing irreversible and reversible oxidation of the element responsible for H_2 production catalysis at potentials higher than 0.2 V vs. SHE in the sterilized and bioactive cathode, respectively. These observations strongly suggest that metallic copper is directly involved in the H_2 catalysis and its significant enhancement, and that its presence on the surface of the electrode is biologically-induced. In the last few years, copper nanoparticles have been reported as efficient electrocatalyst for water electrolysis and the enhancement of the hydrogen evolution reaction.[46-49] Metal copper nanoparticles have attracted much attention for a wide range of applications, including biomedicine, electronics, catalysis and optics and many chemical and physical synthesis methods have been developed and were recently reviewed.[50] Interestingly, microorganisms with the ability to synthetize metal nanoparticles, and in particular metal copper nanoparticles from Cu^{2+}, have also been found.[50-55] The synthetized metal copper nanoparticles were showed to either be secreted extracellularly[51] or stay within the cell wall.[54] The results shown in the present study suggest, for the first time, the bacterial synthesis of metal copper particles modifies the electrode surface and directly contributes to the significant enhancement of hydrogen production. Further research needs to be carried out to confirm these observations and determine whether the copper particles are excreted onto the surface of the cathode, and/or are active from within the cells, and only deposited on the surface after the cells' membrane were broken under extreme conditions. Intracellular copper particles could explain the fast start-up observed after the transfer of an enriched culture in our previous study.[6] Copper-containing hydrogenases could also be considered, but such enzymes would also be denatured by low pH and autoclave treatment. However, one could hypothesize

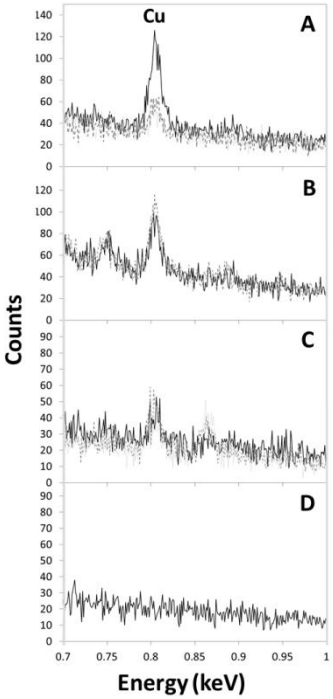

Figure 7. Energy-dispersive X-ray spectroscopy (EDS) spectra, from 0.7 to 1 keV, of (A) and (B) sterilized EPD-3D biocathode duplicates, (C) fully active EPD-3D biocathode and (D) EPD-3D abiotic control.

that the metal centre of such enzyme remained on the surface of the electrode and act alone as catalyst for H_2 production. However, heat treatment was shown to effectively suppress the activity of such extracellular hydrogenases in previous studies.[56] More in-depth investigation of the functions of each enriched microorganisms and of the surface chemistry in different experimental conditions will also need to be assessed.

The novel findings presented in this study are remarkable as they could allow switching from one technology (CO_2 fixation – chemicals production) to the other (hydrogen production) by simply feeding carbon dioxide or not, without performance loss. This could bring biocathode microbial H_2 production at the forefront of BESs potential practical implementation as well. Indeed, the performance of these biocathodes reached H_2 production rates of about 1.15 m^3_{H2} $m^{-2}_{electrode}$ day^{-1} normalized to projected surface area, with a coulombic efficiency of 95 ± 3%. Due to the 3D nature of the electrodes (2620 m^2 m^{-3}), this rate translates to 115 m^3_{H2} $m^{-3}_{electrode}$ day^{-1}. This represents a 27 times increase of the so far highest reported hydrogen production rate (to our knowledge) in microbial electrolysis cells, which used a Ni-based gas diffusion abiotic cathode.[57, 58]

Conclusions

We have demonstrated in this study that the main electron transfer mechanism from the electrode to the terminal electron

acceptor, CO_2, occurs through H_2 and leads to high microbial electrosynthesis rate of acetate. This high H_2 production rate was found to be biologically-induced, most likely through the biological modification of the electrode surface via synthesis of metal copper (nano)-particles. The biofilm was found to be of far greater importance compared to the planktonic cells with the significant enrichment of *Acetoanaerobium*, *Hydrogenophaga* and *Methanobrevibacter.* Indeed, the hydrogen consumers (putatively *Acetoanaerobium*) were shown to be able to utilise a high H_2 flow rate (1.15 m^3_{H2} m^{-2} day^{-1}) within the biofilm, without H_2 able to escape from it. This finding is of critical importance for the potential large-scale implementation of this technology, which allows combining both H_2 production and CO_2 assimilation to an organic final product, within a unique microbial electrosynthesis reactor, without H_2 waste and extra-handling. Finally, we also highlighted the remarkable possibility to switch from organics production technology to pure hydrogen production technology, if desired, by simply stopping the CO_2 feed, without performance loss. In addition, to the best of our knowledge, we report one of the highest H_2 production rate in microbial electrolysis cells configuration. Further in-depth investigations into the microbial processes and the surface chemistry will be needed to fully understand this remarkable electron transfer mechanism.

Experimental Section

BES reactors and operation for microbial enrichment

The fed-batch reactor setup and operation for the enrichment of an active mixed microbial community that is capable of electrosynthesis of acetate from carbon dioxide was described previously.[6, 10] The reactor described in Jourdin et al. (2015) [6], using multi-walled carbon nanotubes synthesized on 45 pores per inch (ppi) reticulated vitreous carbon by electrophoretic deposition as biocathode electrode material (EPD-3D) was used in this current study, after steady performance was reached (about 70 days with cathode chronoamperometrically poised at -0.85 V vs. SHE[6]). An identical reactor with EPD-3D 60 ppi was also used as a duplicate (*i.e.* an electrode with exactly the same nanostructure, but with slightly smaller macropores; only difference between both reactors which doesn't affect the comparisons).

Off-Gas analysis and liquid analysis

The titration and off-gas analysis (TOGA) sensor developed by Gapes et al. (2001) [59] and Pratt et al. (2002) [26] for the study of wastewater treatment systems was modified for this study and is shown in Scheme S1. A pH probe (pH/ORP sensors, Endress + Hauser, Australia) was inserted in the BES reactor and a pH controller (Liquisys M, Endress + Hauser, Australia) was used to control the pH of the cathode (the applied potential was also confirmed not to influence the pH measurements). The cathode medium was recirculated through a smaller bottle (ca. 100 mL liquid volume) using a recirculation pump (Monarch Alloy, TECO Australia Pty Ltd, Australia) with a flow rate of ca. 200 mL min^{-1}. The reactor was additionally stirred with a magnetic stirrer to ensure thorough mixing. The temperature of the liquid phase was also measured using the same probe (pH/ORP sensors, Endress + Hauser, Australia). Both the BES reactor and the recirculation bottle were wrapped with flexible tubing through which water flowed from and to a water bath for the purpose of temperature control. The temperature was controlled at 31 ± 1 °C throughout all the tests. Both the reactor and the recirculation bottle were wrapped in cotton to make temperature control easier and constant throughout the day and all tubing were wrapped in aluminium foil to prevent illumination and phototrophic activity development.

The off-gas measurement technique relies on the use of a quadrupole mass spectrometer (OmniStar, Balzers AG, Liechtenstein) in conjunction with a number of in-line mass flow controllers (MFC) (Bronkhorst Hi-tech, EI-Flow, Netherlands).[26, 59] Helium (Ultra high purity, BOC, Australia) was used as carrier gas and supplied to the reactor via one MFC at a flow rate of 200 mL min^{-1} for each test. Carbon dioxide flow was controlled by another MFC and mixed with the helium flow before being introduced into the reactor for tests in the presence of CO_2. The last MFC was used to control calibration gas flow, which by-passes the reactor and was used for both the calibration of the mass spectrometer and as a baseline during experiments. This premixed gas was supplied from a cylinder (BOC, Australia), and had a defined composition of 2% CO_2, 2% CH_4, 2% H_2, 4% Ar and 90% He. The carrier gas was controlled to provide sufficient stripping driving force, and so that the mass spectrometric intensity signal for the targeted off-gas components (in this case, H_2, CO_2 and CH_4) could be maintained within a narrow range throughout the experiment.[59] During experiments, gas was fed to the recirculation bottle to avoid any disturbance of the cathode electrode in the BES reactor itself. As previously described, humidity was removed from the gas emerging from the recirculation bottle by passing it through a water trap after cooling down the gas through a 4 m copper coiled tube immersed in an cold water bath.[59] The gas was further dried through a drying column where dry air was used to drive moisture out of the gas across a membrane, prior to sampling by the mass spectrometer. The majority of the off-gas was vented prior to measurement, reducing pressure fluctuations at the mass spectrometer capillary inlet.[59]

For the calibration of the mass spectrometer, the carrier gas (with or without CO_2, BOC, Australia) depending on whether it was used for the test) was sparged, at the same flows as used for the experiment (200 mL min^{-1}), through a calibration bottle instead, which had the same volume as the recirculation bottle and was filled with the same catholyte solution as described above. Different flows of the calibration gas were used to obtain regression lines for each targeted gas. Deviation of the signals over the time of the experiment was taken into account by performing a calibration before and after each experiment. Argon, an inert gas, was used as an internal standard. The flow rates of the targeted gases (H_2, CH_4, CO_2) were then determined by measuring the change in their concentration relative to the argon gas concentration and mass flow rate.[26]

The measured flow-rates of H_2 in mL min^{-1} were converted in mol of H_2 using the ideal gas law and further converted into mA (i.e. current assimilated into H_2) using Faraday's law, which is the final H_2 form plotted and referred to in the Results and Discussion section.

The concentrations of volatile fatty acids (VFA) in the liquid phase were determined by a gas chromatography method.[10]

Electrochemical-TOGA tests

After the reactor was installed on the TOGA sensor setup, a cathode potential of -0.85 V vs. SHE was applied over a period of 87 days (current density evolution can be seen in Figure S5) and only momentarily stopped, as indicated in the text, to perform linear sweep voltammetry tests. A multi-channel potentiostat (VMP-3, Bio-Logic SAS, France) was used for all experiments. It has to be stressed here that the

TOGA sensor could not be used at all times for online gas measurement, but the same recirculation setup was used and the potentiostatic measurements were carried out at all times nevertheless. For each test with CO_2 that was performed, CO_2 was mixed with the carrier gas at a flow rate of 70 mL min^{-1} (soluble CO_2/HCO_3^- in excess, to prevent limitation and study electron fluxes).

- Electron flux investigation

To investigate the electron fluxes and elucidate possible syntrophic interactions within the cathodic microbial community, different tests were performed with the TOGA sensor. Chronoamperometry experiments with the cathode potential poised at -0.85 V vs. SHE both with and without carbon dioxide fed, respectively) were performed, at constant pH of 6.7. Liquid samples for VFA analysis were taken at the beginning and at the end of each test. Additionally, linear sweep voltammetry (LSV) at pH 6.7 both in the presence and absence of CO_2 were performed around day 30 to 35. The potential was scanned from 0 to -1.0 V vs. SHE, unless otherwise specified, at a scan rate of 0.1 mV s^{-1}. Chronoamperometry and LSV tests with the TOGA sensor and in the exact same conditions were also carried out on an abiotic control equipped with the same cathode material (EPD-3D-45 ppi), without an inoculum addition, for comparison with the biocathode performance.

- Biofilm / planktonic cells relative importance to MES performance

The respective importance of both biofilm and planktonic cells on acetate production rate was assessed by replacing the whole of the cathode medium with fresh cell-free medium, and performing chronoamperometry at -0.85 V vs. SHE; liquid samples were taken at the start and end of each test.

- Biofilm removal

We further investigated the role of the biofilm on the MES performance. To do so, the system underwent several extreme conditions in order to remove the biofilm. Firstly, the pH was decreased to 2 for 2-3 hours, then the reactor and recirculation bottle were autoclaved while the rest of the setup was sterilized with EtOH, and finally, the electrode was taken out and air-dried for a week. After each treatment, the electrode was reconnected and current recorded at the same applied potential of -0.85 V vs. SHE. The duplicate reactor underwent the low pH and autoclave treatment only.

Scanning Electron Microscopy (SEM) – Energy-Dispersive X-ray Spectroscopy (EDS)

Electrode samples from both active biocathode and sterilized reactors were fixed in 5% glutaraldehyde for 2 h. The samples then underwent a MilliQ® water postfix wash. Dehydrated (<24 h in a high vacuum desiccator) and subsequently carbon coated (QT150TS Turbo-pumped coater, Argon purged) samples were imaged in secondary electron mode, and EDS data collected, employing a XL30 Philips conventional (LaB6 source electron gun) Scanning Electron Microscope. Samples were imaged at 20 kV acceleration, 10–12 mm working distance and 6.0 spot size.

Fluorescent in situ hybridization (FISH)

Small amounts of biofilm removed from the electrode surface were first fixed with 4% paraformaldehyde (PFA) for two hours and then washed with phosphate buffered saline (PBS, 130mM sodium chloride, 10mM sodium phosphate buffer, pH 7.2) and stored at 1:1 100% ethanol: PBS. FISH was performed according to the protocol described by Manz et al. (1993).[60] Details of the oligonucleotides FISH probes used are listed in Table S1. The microscope slides were viewed under Zeiss Axioscope LSM510 confocal microscope (Zeiss, Germany).

Microbial community analysis

Biofilm and planktonic cells were collected from two replicate biocathodes under steady MES performance. Those reactors were started using the same inoculum and electrode materials as described above and reached the same performance (data not shown) as the other reactors described here. Genomic DNA was separately extracted with FastDNA SPIN Kit for Soil (MP Biomedicals, Santa Ana, California, US) according to manufacturer's protocol. 300 ng DNA of each sample were provided to the Australian Centre for Ecogenomics (ACE) for 16S rRNA Amplicon paired-end sequencing by Illumina Miseq Platform using 926F (5'-AAACTYAAAKGAATTGACGG-3') and 1392wR (5'-ACGGGCGGTGWGTRC-3') primer set.[61]

Raw paired reads was first trimmed by Trimmomatic[62] to remove short reads (less than 190bp) and low quality (lower than Phred-33 of 20). The trimmed paired reads were then assembled by Pandaseq[63] with default parameters. The adapter sequences were removed by FASTQ Clipper of FASTX-Toolkit.[64] The joined high quality sequences was analysed by QIIME v1.8.0[65] using open-reference OTU picking strategy by uclust[66] at 1% phylogenetic distance and assigned taxonomy by uclust against greengenes database (13_05 release[67, 68]). OTUs with only one read were filtered from the OTUs table by command filter_otus_from_otu_table.py in QIIME. In house script "Normaliser" (https://github.com/minillinim/Normaliser) was used to find a centroid normalized OTUs table with 40000 reads per sample.

Acknowledgements

VF acknowledges a UQ Postdoctoral Fellowship. This work was supported by the Australian Research Council Grant DP110100539. The authors acknowledge the facilities and the scientific and technical assistance of the Australian Microscopy & Microanalysis Research Facility at the Centre for Microscopy and Microanalysis (The University of Queensland). The authors also acknowledge the facilities, and the scientific and technical assistance, of the Australian Centre for Ecogenomics (the University of Queensland) for pyrosequencing analysis. The authors thank Dr. B. C. Donose for fruitful discussions and SEM imaging of the biofilm samples. The authors also acknowledge Dr. J. Chen and the ARC Centre of Excellence for Electromaterials Science, University of Wollongong, NSW, Australia, for providing EPD-3D electrodes.

Keywords: Microbial electrosynthesis • Carbon dioxide fixation • Biohydrogen • Electron transfer • Biofilm

[1] K. Rabaey, R. A. Rozendal *Nat Rev Micro*. **2010**, 8, 706-716.

[2] R. Ganigue, S. Puig, P. Batlle-Vilanova, M. D. Balaguer, J. Colprim *Chemical Communications*. **2015**, 51, 3235-3238.

[3] M. Mikkelsen, M. Jørgensen, F. C. Krebs *Energy and Environmental Science*. **2010**, 3, 43-81.

[4] D. R. Lovley, K. P. Nevin *Current Opinion in Biotechnology*. **2013**, 24, 385-390.
[5] K. P. Nevin, T. L. Woodard, A. E. Franks, Z. M. Summers, D. R. Lovley *mBio*. **2010**, 1, 1-4.
[6] L. Jourdin, T. Grieger, J. Monetti, V. Flexer, S. Freguia, Y. Lu, J. Chen, M. Romano, G. G. Wallace, J. Keller *Environmental Science & Technology*. **2015**.
[7] P. Batlle-Vilanova, S. Puig, R. Gonzalez-Olmos, M. D. Balaguer, J. Colprim *Journal of Chemical Technology & Biotechnology*. **2015**.
[8] N. Xafenias, V. Mapelli *International Journal of Hydrogen Energy*. **2014**, 39, 21864-21875.
[9] E. V. LaBelle, C. W. Marshall, J. A. Gilbert, H. D. May *PLoS ONE*. **2014**, 9, e109935.
[10] L. Jourdin, S. Freguia, B. C. Donose, J. Chen, G. G. Wallace, J. Keller, V. Flexer *Journal of Materials Chemistry A*. **2014**, 2, 13093-13102.
[11] T. Zhang, H. Nie, T. S. Bain, H. Lu, M. Cui, O. L. Snoeyenbos-West, A. E. Franks, K. P. Nevin, T. P. Russell, D. R. Lovley *Energy & Environmental Science*. **2013**, 6, 217-224.
[12] S. Min, Y. Jiang, D. Li *Journal of Microbiology and Biotechnology*. **2013**, 23, 1140-1146.
[13] C. W. Marshall, D. E. Ross, E. B. Fichot, R. S. Norman, H. D. May *Environmental Science and Technology*. **2013**, 47, 6023-6029.
[14] C. W. Marshall, D. E. Ross, E. B. Fichot, R. S. Norman, H. D. May *Applied and Environmental Microbiology*. **2012**, 78, 8412-8420.
[15] K. P. Nevin, S. A. Hensley, A. E. Franks, Z. M. Summers, J. Ou, T. L. Woodard, O. L. Snoeyenbos-West, D. R. Lovley *Applied and Environmental Microbiology*. **2011**, 77, 2882-2886.
[16] L. Jourdin, S. Freguia, B. C. Donose, J. Keller *Bioelectrochemistry*. **2015**, 102, 56-63.
[17] S. A. Patil, J. B. A. Arends, I. Vanwonterghem, J. van Meerbergen, K. Guo, G. W. Tyson, K. Rabaey *Environmental Science & Technology*. **2015**, 49, 8833-8843.
[18] C. G. S. Giddings, K. Nevin, T. Woodward, D. R. Lovley, C. S. Butler *Frontiers in Microbiology*. **2015**, 6.
[19] G. Mohanakrishna, J. S. Seelam, K. Vanbroekhoven, D. Pant *Faraday Discussions*. **2015**.
[20] S. Bajracharya, A. ter Heijne, X. D. Benetton, K. Vanbroekhoven, C. J. Buisman, D. P. Strik, D. Pant *Bioresource Technology*. **2015**.
[21] U. Schroder *Physical Chemistry Chemical Physics*. **2007**, 9, 2619-2629.
[22] L. Huang, J. M. Regan, X. Quan *Bioresource Technology*. **2011**, 102, 316-323.
[23] D. R. Lovley *Environmental Microbiology Reports*. **2011**, 3, 27-35.
[24] M. Rosenbaum, F. Aulenta, M. Villano, L. T. Angenent *Bioresource Technology*. **2011**, 102, 324-333.
[25] E. Blanchet, F. Duquenne, Y. Rafrafi, L. Etcheverry, B. Erable, A. Bergel *Energy & Environmental Science*. **2015**, 8, 3731-3744.
[26] S. Pratt, Z. Yuan, D. Gapes, M. Dorigo, R. J. Zeng, J. Keller *Biotechnology and Bioengineering*. **2002**, 81, 482-495.
[27] S. Freguia, K. Rabaey, Z. Yuan, J. Keller *Environmental Science & Technology*. **2007**, 41, 2915-2921.
[28] R. A. Rozendal, H. V. M. Hamelers, G. J. W. Euverink, S. J. Metz, C. J. N. Buisman *International Journal of Hydrogen Energy*. **2006**, 31, 1632-1640.
[29] A. W. Jeremiasse, H. V. M. Hamelers, C. J. N. Buisman *Bioelectrochemistry*. **2010**, 78, 39-43.
[30] R. A. Rozendal, A. W. Jeremiasse, H. V. M. Hamelers, C. J. N. Buisman *Environmental Science and Technology*. **2008**, 42, 629-634.
[31] R. Sleat, R. A. Mah, R. Robinson *International Journal of Systematic Bacteriology*. **1985**, 35, 10-15.
[32] A. WILLEMS, J. BUSSE, M. GOOR, B. POT, E. FALSEN, E. JANTZEN, B. HOSTE, M. GILLIS, K. KERSTERS, G. AULING, J. DE LEY *International Journal of Systematic Bacteriology*. **1989**, 39, 319-333.
[33] Z.-i. Kimura, S. Okabe *The Journal of General and Applied Microbiology*. **2013**, 59, 261-266.
[34] Z. I. Kimura, S. Okabe *ISME Journal*. **2013**, 7, 1472-1482.
[35] C.-Y. Lai, X. Yang, Y. Tang, B. E. Rittmann, H.-P. Zhao *Environmental Science & Technology*. **2014**, 48, 3395-3402.
[36] H. Park, Y.-J. Choi, D. Pak *Biotechnology Letters*. **2005**, 27, 949-953.
[37] F. A. Armstrong, J. Hirst *Proceedings of the National Academy of Sciences*. **2011**, 108, 14049-14054.
[38] U. Deppenmeier, V. Müller in *Life close to the thermodynamic limit: how methanogenic archaea conserve energy, Vol.*, Springer, **2008**, pp.123-152.
[39] J. Yu *Trends in Biotechnology*. **2014**, 32, 5-10.
[40] B.-J. Ni, H. Liu, Y.-Q. Nie, R. J. Zeng, G.-C. Du, J. Chen, H.-Q. Yu *Biotechnology and Bioengineering*. **2011**, 108, 345-353.
[41] F. Zhang, J. Ding, Y. Zhang, M. Chen, Z.-W. Ding, M. C. M. van Loosdrecht, R. J. Zeng *Water Research*. **2013**, 47, 6122-6129.
[42] B. S. Kim, S. C. Lee, S. Y. Lee, H. N. Chang, Y. K. Chang, S. I. Woo *Biotechnology and Bioengineering*. **1994**, 43, 892-898.
[43] K. Tanaka, A. Ishizaki, T. Kanamaru, T. Kawano *Biotechnology and Bioengineering*. **1995**, 45, 268-275.
[44] K. P. Nevin, B. C. Kim, R. H. Glaven, J. P. Johnson, T. L. Woodward, B. A. Methé, R. J. Didonato Jr, S. F. Covalla, A. E. Franks, A. Liu, D. R. Lovley *PLoS ONE*. **2009**, 4, 1-11.
[45] B. Beverskog, I. Puigdomenech *Journal of The Electrochemical Society*. **1997**, 144, 3476-3483.
[46] J. Ahmed, P. Trinh, A. M. Mugweru, A. K. Ganguli *Solid State Sciences*. **2011**, 13, 855-861.
[47] E. Aslan, I. H. Patir, M. Ersoz *Chemistry – A European Journal*. **2015**, n/a-n/a.
[48] B. Kumar, S. Saha, M. Basu, A. K. Ganguli *Journal of Materials Chemistry A*. **2013**, 1, 4728-4735.
[49] C. C. Văduva, N. Vaszilcsin, A. Kellenberger, M. Medeleanu *International Journal of Hydrogen Energy*. **2011**, 36, 6994-7001.
[50] B. Khodashenas, H. R. Ghorbani *Korean Journal of Chemical Engineering*. **2014**, 31, 1105-1109.
[51] R. Ramanathan, M. R. Field, A. P. O'Mullane, P. M. Smooker, S. K. Bhargava, V. Bansal *Nanoscale*. **2013**, 5, 2300-2306.
[52] O. Rubilar, M. Rai, G. Tortella, M. C. Diez, A. B. Seabra, N. Durán *Biotechnology Letters*. **2013**, 35, 1365-1375.
[53] S. Saif Hasan, S. Singh, R. Y. Parikh, M. S. Dharne, M. S. Patole, B. Prasad, Y. S. Shouche *Journal of nanoscience and nanotechnology*. **2008**, 8, 3191-3196.
[54] M. R. Salvadori, R. A. Ando, C. A. O. do Nascimento, B. Corrêa *PLoS ONE*. **2014**, 9, e87968.
[55] S. Shantkriti, P. Rani *Int. J. Curr. Microbiol. App. Sci*. **2014**, 3, 374-383.
[56] J. S. Deutzmann, M. Sahin, A. M. Spormann *mBio*. **2015**, 6.
[57] A. Kundu, J. N. Sahu, G. Redzwan, M. A. Hashim *International Journal of Hydrogen Energy*. **2013**, 38, 1745-1757.
[58] M. F. Manuel, V. Neburchilov, H. Wang, S. R. Guiot, B. Tartakovsky *Journal of Power Sources*. **2010**, 195, 5514-5519.
[59] D. Gapes, J. Keller *Biotechnology and Bioengineering*. **2001**, 76, 361-375.
[60] W. Manz, U. Szewzyk, P. Ericsson, R. Amann, K. H. Schleifer, T. A. Stenström *Applied and Environmental Microbiology*. **1993**, 59, 2293-2298.
[61] A. Engelbrektson, V. Kunin, K. C. Wrighton, N. Zvenigorodsky, F. Chen, H. Ochman, P. Hugenholtz *The ISME journal*. **2010**, 4, 642-647.
[62] A. M. Bolger, M. Lohse, B. Usadel *Bioinformatics*. **2014**, btu170.
[63] A. P. Masella, A. K. Bartram, J. M. Truszkowski, D. G. Brown, J. D. Neufeld *BMC bioinformatics*. **2012**, 13, 31.
[64] W. R. Pearson, T. Wood, Z. Zhang, W. Miller *Genomics*. **1997**, 46, 24-36.
[65] J. G. Caporaso, J. Kuczynski, J. Stombaugh, K. Bittinger, F. D. Bushman, E. K. Costello, N. Fierer, A. G. Pena, J. K. Goodrich, J. I. Gordon *Nature methods*. **2010**, 7, 335-336.
[66] R. C. Edgar *Bioinformatics*. **2010**, 26, 2460-2461.
[67] D. McDonald, M. N. Price, J. Goodrich, E. P. Nawrocki, T. Z. DeSantis, A. Probst, G. L. Andersen, R. Knight, P. Hugenholtz *The ISME journal*. **2012**, 6, 610-618.

[68] J. J. Werner, O. Koren, P. Hugenholtz, T. Z. DeSantis, W. A. Walters, J. G. Caporaso, L. T. Angenent, R. Knight, R. E. Ley *The ISME journal*. **2012**, 6, 94-103.

Entry for the Table of Contents

FULL PAPER

High CO_2 fixation rate in the sole form of acetate by microbial electrosynthesis was demonstrated to be driven by biologically-induced hydrogen and to occur exclusively within the biofilm, at zero wastage of hydrogen

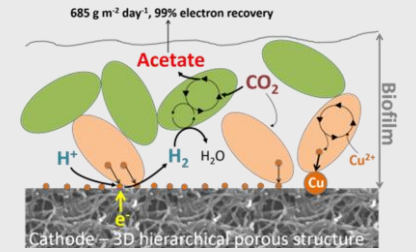

*Ludovic Jourdin,[*a,b,†] Yang Lu,[a] Victoria Flexer,[a,‡] Jurg Keller,[*a] and Stefano Freguia[a,b]*

Page No. – Page No.

Biologically-induced hydrogen production drives high rate / high efficiency microbial electrosynthesis of acetate from carbon dioxide